THE JOURNAL OF BIOLOGICAL CHEMISTRY VOL. 284, NO. 5, pp. 2880–2890, January 30, 2009
© 2009 by The American Society for Biochemistry and Molecular Biology, Inc. Printed in the U.S.A.

α- and γ-Protocadherins Negatively Regulate PYK2*

Received for publication, September 24, 2008, and in revised form, December 1, 2008 Published, JBC Papers in Press, December 1, 2008, DOI 10.1074/jbc.M807417200

Jian Chen[1], **Yanyan Lu, Shuxia Meng, Meng-Hsuan Han, Chengyi Lin, and Xiaozhong Wang**[2]

From the Department of Biochemistry, Molecular Biology and Cell Biology, Northwestern University, Evanston, Illinois 60208

Genetic studies demonstrate that γ-protocadherins (PCDH-γ) are required for the survival and synaptic connectivity in neuronal subpopulations of the central nervous system. However, the intracellular signaling mechanisms for PCDH-γ are poorly understood. Here, we show that PCDH-γ binds two tyrosine kinases, PYK2 and focal adhesion kinase (FAK), and interaction with PCDH-γ inhibits kinase activity. Consistent with this, PYK2 activity is abnormally up-regulated in the *Pcdh-γ*-deficient neurons. Overexpression of PYK2 induces apoptosis in the chicken spinal cord. Thus, negative regulation of PYK2 activity by PCDH could contribute to the survival of subsets of neurons. Surprisingly, we found that PCDH-α interacts similarly with PYK2 and FAK despite containing a distinct cytoplasmic domain. In neural tissue, PCDH-γ, together with PCDH-α, forms functional complexes with PYK2 and/or FAK. Therefore, the identification of common intracellular effectors for PCDH-γ and PCDH-α suggests that dozens of protocadherins generated by *Pcdh-α* and *Pcdh-γ* gene clusters can converge different extracellular signals into common intracellular pathways.

Cadherin superfamily molecules have evolved to play an instructive role in cell-cell interactions during tissue morphogenesis in multicellular organisms (1–3). Nearly 80 different protocadherin genes constitute the largest group within the cadherin superfamily. Like classic cadherins, protocadherins usually share similar structural organization in their extracellular domains with six or more ectodomain repeats but have divergent cytoplasmic domains. Among protocadherins, three families of α-, β-, and γ-protocadherin genes (designated *Pcdh-α*, *Pcdh-β*, and *Pcdh-γ*) are arrayed in tandem on a single chromosome (4). The overall genomic organization of these gene families is conserved in all vertebrates (5, 6). For the PCDH-α or PCDH-γ family, each PCDH isoform contains distinct extracellular and transmembrane domains encoded by one large variable exon. By contrast, all isoforms within a family contain a common cytoplasmic domain encoded by three constant exons. Individual neurons express a combination of PCDH-α and PCDH-γ isoforms through differential promoter activation and alternative splicing (7–11), with the majority of PCDH-α and PCDH-γ isoforms (C-type isoforms excluded) expressed monoallelically (12, 13). One possibility is that cell-specific PCDH expression patterns are enforced through allelic exclusion as a result of competition for shared long range regulatory elements (14). PCDH proteins appear to have adhesive activity (8, 15) and are predominantly expressed in the neuronal tissues throughout development. PCDH proteins have been shown to be associated with synapses and intracellular vesicles (7, 16–18). Genetic analyses of mice lacking the entire *Pcdh-γ* gene cluster (*Pcdh-γ$^{del/del}$*) provided evidence that PCDH-γ is essential for neural development (16). During late embryonic development, dramatic apoptosis and synaptic loss in the spinal interneurons led to neonatal lethality. Further analysis of *Pcdh-γ$^{del/del}$*; *Bax$^{-/-}$* mutant mice in which apoptosis is circumvented revealed a decrease of both excitatory and inhibitory synapses in the spinal cord (19). More recently, an abnormality in axon convergence of olfactory sensory neurons has been observed in *Pcdh-α$^{-/-}$* mice (20). Collectively, these data suggest that PCDH proteins play a role in establishing neuronal connectivity via regulation of cell adhesion and cell death.

An important remaining question is how PCDH function interfaces with cell signaling pathways during development. The 22 mouse PCDH-γ isoforms share a common cytoplasmic domain, and their extracellular domains are distinct and diverse, thus suggesting a potential mechanism of PCDH-γ action-signal convergence through the common intracellular domain. Mice expressing C-terminal truncated PCDH-γ proteins (*Pcdh-γ$^{tru/tru}$*) displayed neonatal lethality and spinal interneuron phenotypes similar to *Pcdh-γ$^{del/del}$*; *Bax$^{-/-}$* mice, suggesting that the intracellular domain is essential for PCDH-γ function *in vivo* (19). There are two prominent models that explain PCDH intracellular function. First, the intracellular tail of PCDH might act directly as a regulator of transcription in a manner similar to Notch signaling. Consistent with this view, the intracellular domain of PCDH-γs is proteolytically processed by metalloproteinases and γ-secretases (21, 22), and the cleaved cytoplasmic domain localizes in the nucleus and activates the transcription of *Pcdh-γ* in transfected nonneuronal cells (22). Second, the intracellular tail might function as a docking site for cytoplasmic signaling transducers. However, currently, evidence supporting a signaling mechanism has not been reported.

As an initial test of these two models, we used a modified two-hybrid screen to identify proteins that bind the cytoplasmic tail of PCDH-γ. Here, we report that two members of the focal adhesion kinase (FAK)[3] family, PYK2 and FAK, directly

* This work was supported, in whole or in part, by National Institutes of Health Grant 5R01NS051253 (to X. W.). The costs of publication of this article were defrayed in part by the payment of page charges. This article must therefore be hereby marked "*advertisement*" in accordance with 18 U.S.C. Section 1734 solely to indicate this fact.

[1] Present address: Yantai Yuhuangding Hospital, Qingdao University, Yantai 264000, Shandong, China.

[2] To whom correspondence should be addressed: Dept. of Biochemistry, Molecular Biology, and Cell Biology, Northwestern University, 2205 Tech Dr., Hogan 2-100, Evanston, IL 60208-3500. Tel.: 847-467-4897; Fax: 847-467-1380; E-mail: awang@northwestern.edu.

[3] The abbreviations used are: FAK, focal adhesion kinase; GST, glutathione *S*-transferase; BrdUrd, 5′-bromo-2′-deoxyuridine; IP, immunoprecipitation; PSD, postsynaptic density; NCAM, neural cell adhesion molecule; GFP, green fluorescent protein.

interact with the common cytoplasmic domain of PCDH-γ. We also found that PCDH-α interacts with these intracellular kinases. PCDH-γ, PCDH-α, FAK, and PYK2 are present in large membrane protein complexes in neural tissue. Interaction with PCDH-γ and PCDH-α inhibits FAK and PYK2 activity *in vitro* and *in vivo*, and PYK2 activity is up-regulated in PCDH-γ-deficient mice. Furthermore, overexpression of PYK2 leads to an increase of apoptosis in the developing chicken spinal cord. Therefore, negative regulation of the proapoptotic activity of PYK2 by protocadherins could play a role in maintaining neuronal survival during development.

EXPERIMENTAL PROCEDURES

CytoTrap Two-hybrid Screen—We used the yeast CytoTrap two-hybrid system from Stratagene to identify PCDH-γC-interacting proteins (23). To construct γC bait, we PCR-amplified the cDNA encoding γC domain without the last 10-amino acid sequence with primer 936 (5′-CCT CCG TCG ACG CAG CAA GCC CCG CCC AA-3′) and 939 (5′-AGC AAG CTT GCG GCC GCT TAG TTG CCA TTA CCA CCT GCT GG-3′). After digestion with SalI and NotI, γC cDNA was cloned into *pSOS* and used as bait. We screened a mouse adult brain cDNA library from Stratagene according to the manufacturer's instructions.

cDNA Expression Vector Construction—The expression vectors for a variety of *Pcdh-γ*, *Pcdh-α*, FAK, and *PYK2* cDNAs were constructed by cloning restriction enzyme-digested or PCR-amplified DNA fragments into *pGEX.KG*, *pcDNA3* (Invitrogen), *p3×FLAG-CMV-9/10* (Sigma), and *PB-CAG*. Different epitope tags, including 9E10-myc, FLAG, and V5, were used to tag individual cDNAs. The kinase-dead *PYK2* and *FAK* vectors with point mutations (*pB-CAG-V5-PYK2 Y402F*; *K457A* and *pB-CAG-V5-FAK Y397F*; *K454R, Y620*; *Y621F*) were generated by overlapping PCR followed by restriction enzyme-based cloning. The original full-length human *PYK2* and mouse *FAK* cDNAs were obtained from IMAGE or FANTOM clone collections. All cloning and mutagenesis were verified by complete or partial sequencing.

GST Pull-down, Immunoprecipitation, and in Vitro Kinase Assay—Bacterially expressed GST fusion proteins were expressed and purified as previously described (16). GST-γC, GST-αC, GST-N-Cad-C, and GST alone were used in this study. For pull-down assays, aliquots of immobilized GST proteins (10–15 μg) were used to incubate with 293T cell lysates that expressed different PCDH, PYK2, and FAK proteins. The lysates were prepared in a lysis buffer (50 mM Tris, pH 7.5, 150 mM NaCl, 1.0% Nonidet P-40, 10% glycerol, 1.5 mM $MgCl_2$, 1 mM EDTA, 0.2 mM EGTA, 20 mM NaF, 25 μM $ZnCl_2$, 1 mM Na_3VO_4, 1 mM phenylmethylsulfonyl fluoride, and Roche Applied Science protease inhibitors). After incubation and washing, the pull-down proteins were detected by Western blot.

Immunoprecipitation from cultured cells were carried out as previously described with modifications (24). A variety of FLAG-tagged proteins were expressed in 293T or SYF cells, lysed in the same lysis buffer described above, and purified with anti-FLAG M2 affinity gel (Sigma). Insect cell-expressed GST-tagged FAK and His-tagged PYK2 proteins were purchased from Invitrogen and Millipore, respectively. For affinity purification of PCDH-γ-GFP complexes from the brain, the crude membrane proteins were first prepared as described before (16). In brief, the whole brain tissues were homogenized with a tissue grinder in the buffer (50 mM Tris, pH 7.5, 150 mM NaCl, 1 mM EDTA, 10 mM NaF, 10 mM Na_3VO_4, 1 mM phenylmethylsulfonyl fluoride, and Roche Applied Science protease inhibitors). The cell debris and nuclei were removed by low speed centrifugation, and the crude membrane proteins were harvested by high speed (16,000 rpm) centrifugation in a microcentrifuge for 20 min. The resulted membrane proteins were then suspended in the buffer (50 mM Tris, pH 7.5, 150 mM NaCl, 1 mM EDTA, 10 mM NaF, 10 mM Na_3VO_4, 1 mM phenylmethylsulfonyl fluoride, 0.8% Triton X-100, and protease inhibitors). After a 20-min high speed (16,000 rpm) centrifugation and preabsorption with bovine serum albumin-saturated Sepharose beads for 30 min, the PCDH-γ-GFP complexes were isolated with anti-GFP-agarose beads (MBL).

In vitro kinase assays were carried out as previously described (24). In brief, immunopurified kinases were incubated with exogenous substrate, E4Y1 polypeptide from Sigma, in a kinase buffer (50 mM Tris, pH 7.4, 10 mM $MnCl_2$, 20 μCi of [γ-^{32}P]ATP, and 10 μg of E4Y1) for 20 min at 37 °C. Various amounts of GST proteins (0–5 μg) were added to measure their effect on kinase activity.

Cell Culture, Primary Neuron Culture, and Transfection—Human kidney HEK 293T and SYF fibroblasts were originally purchased from ATCC and cultured in Dulbecco's modified Eagle's medium with 10% fetal calf serum. Lipofectamine 2000 (Invitrogen) was used in all transfection experiments. Primary neuron cultures were prepared from E18 *Pcdh-γ^{fusg}* mouse hippocampi essentially as in Brewer *et al.* (25). Briefly, neurons were plated at a density of 3.6×10^4 cells/cm^2 on (0.002%) poly-L-lysine-coated coverslips. Neurons were maintained in Neurobasal with B27 supplements for 2 weeks and processed for immunocytochemistry.

Antibodies—The antibodies used in the study were from the following sources: mouse anti-FLAG M2 (Sigma); rabbit anti-GFP (Invitrogen); rat anti-GFP beads (MBL); rat anti-GFP antibody (MBL); rabbit anti-FAK (Upstate and Cell Signaling); mouse anti-FAK (Upstate); rabbit anti-Tyr(P)^{397}-FAK (BIOSOURCE); rabbit anti-PYK2 (Upstate and Abcam); mouse anti-PYK2 (BD Biosciences); rabbit anti-Tyr(P)^{402}-PYK2 (BIOSOURCE); 9E10 anti-Myc (DSHB); E7 anti-β-tubulin (DSHB); rabbit anti-synapsin I (Invitrogen); mouse anti-pan-cadherin (Sigma); mouse anti-NF200 (Sigma); rat anti-BrdUrd (Accurate Chemical and Scientific); mouse anti-V5 (Invitrogen and Serotec); rabbit anti-phosphohistone H3 (Cell Signaling); rabbit anti-cleaved caspase-3 (Cell Signaling); and secondary antibodies (Invitrogen, Jackson ImmunoResearch Laboratories, and Santa Cruz Biotechnology, Inc. (Santa Cruz, CA)). Rabbit anti-N-CAM and rabbit anti-PCDH-γ were previously generated. The specificity of PCDH-γ antibody was previously characterized by Western blot on brain lysates from knock-out mice (16). The rabbit anti-PCDH-α was generated in this study, and the specificity on brain lysates was confirmed by mass spectrometry identification in a related study. The specificity of

FAK and PYK2 antibodies was verified by at least two or three different commercially available antibodies.

Fractionation and Sucrose Gradient Ultracentrifugation—The fractionation of total brain proteins was described by Carlin *et al.* (26). In brief, the brain homogenate was first clarified by low speed (700 × *g*) centrifugation, and the supernatant was then separated into the soluble cytosolic fraction (S2) and pellet (crude membrane P2) by high speed centrifugation (13,800 × *g*). The resulting crude membrane proteins were further fractionated by discontinuous sucrose gradient ultracentrifugation (82,500 × *g*). The synaptosome fraction was collected from the interface between 1.0 and 1.2 M sucrose layers. The Triton X-100-insoluble postsynaptic density (PSD) fraction was collected as a pellet after the following ultracentrifugation.

For sucrose gradient ultracentrifugation, whole brain tissues were homogenized using a tissue grinder. Tissue debris and nuclei were removed by centrifugation at 500 × *g* for 10 min. The water-insoluble fraction in the supernatant was collected by centrifugation at 26,000 × *g* for 20 min. Total water-insoluble proteins were extracted in the same buffer with 2% Triton X-100 and clarified by centrifugation at 26,000 × *g* for 20 min. The Triton X-100-extracted proteins were then separated on a 5–50% sucrose gradient at 33,000 rpm in a SW41Ti rotor at 4 °C for 17.5 h. 750-μl fractions were collected from the top. Aliquots of individual fractions that contained an equal amount of proteins were resolved by SDS-PAGE and analyzed by Western blot. Bovine serum albumin (66 kDa), thyroglobulin (669 kDa), and blue dextran (2,000 kDa) were used as size standards for sucrose gradient ultracentrifugation. The peak of the PCDH-γ complexes lies around 600 kDa. The protein concentration in each fraction was first determined by a BCA protein assay kit from Pierce, and the equal loading of proteins from two genotypes was then confirmed by Coomassie staining of SDS-polyacrylamide gels. The SDS-PAGE and Western blotting were conducted in identical gels, transferred, probed, with antibodies, and developed with ECL at the same time. The Western blot results were reproduced at least three times.

In Ovo Electroporation of Chick Spinal Cord—Fertilized white leghorn chicken eggs were incubated at 38 °C to stage 12 by Hamburger and Hamiltons' criteria prior to electroporation. DNA mixtures of both V5-PYK2-expressing PB transposon and PB transposase were injected into the central canal of the neural tube, and electroporation was performed in the thoracic segment of the spinal cord as previously described (27). For BrdUrd labeling, 50 μl of BrdUrd (Sigma; 100 mM in phosphate-buffered saline) were dropped on chicken embryos, and embryos were incubated for 1 h before harvesting.

RESULTS

PCDH-γ Interacts with PYK2 and FAK in Vitro—To investigate the intracellular signaling mechanism of PCDH-γ, we employed a yeast CytoTrap two-hybrid screen to identify proteins that interact with the shared cytoplasmic domain of PCDH-γ (γC). The CytoTrap system relies on the ability of the human SOS protein to rescue a temperature-sensitive yeast mutant in the Ras signaling pathway when localized in the proximity of plasma membrane. The bait we used is a fusion protein between human SOS and the first 115 amino acids in γC. The last 10 amino acids of γC were deleted, because the bait containing this sequence had a background activity in the CytoTrap system. We screened 2 × 10^6 clones from a mouse adult brain cDNA library and identified 20 different candidate proteins that specifically interacted with pSOS-γC bait. One positive clone encodes an in-frame fusion between the myristoylation signal and N-terminal truncated PYK2 (amino acids 364–967 of mouse proline-rich tyrosine kinase 2) (28). Since PYK2 and FAK share significant sequence homology, we tested both full-length PYK2 and FAK for their interactions with the bait pSOS-γC. As shown in Fig. 1*A*, pSOS-γC specifically interacted with both pMyr-PYK2 and pMyr-FAK and rescued the growth of temperature-sensitive yeast at 37 °C. To determine if γC could bind to PYK2 or FAK, we purified a bacterially expressed GST fusion protein containing the entire shared cytoplasmic domain of PCDH-γ (GST-γC, including the last 10 amino acids that were excluded in the CytoTrap) and tested for its binding

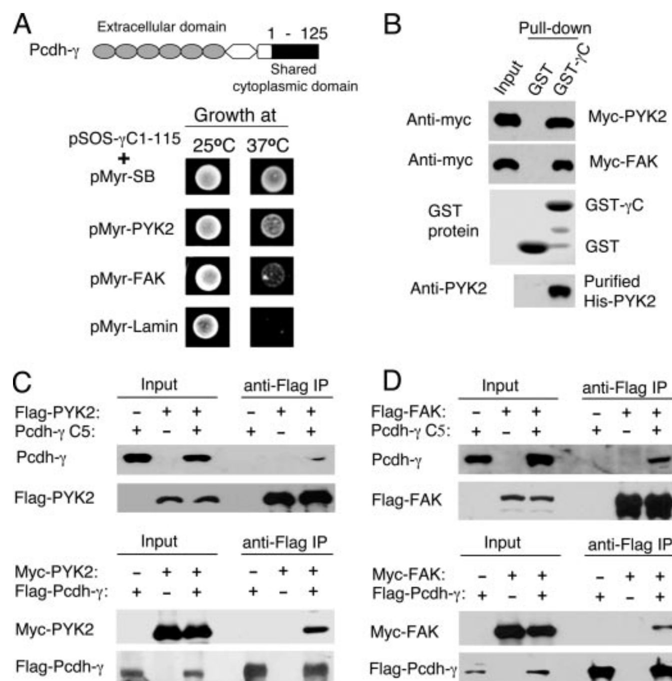

FIGURE 1. **PCDH-γ interacts with PYK2 and FAK *in vitro*.** *A*, a schematic of the domain structure of PCDH-γ protein. The shared cytoplasmic domain of PCDH-γ (γC; 125 amino acids) is marked. γC (amino acids 1–115) interacts with PYK2 and FAK in the yeast CytoTrap two-hybrid system. Cotransformation of the bait pSOS-γC with pMyr-PYK2 and pMyr-FAK into the *cdc25H* strain showed that both pMyr-PYK2 and pMyr-FAK interacted with pSOS-γC and rescued yeast growth defect at a restrictive temperature of 37 °C. pMyr-SB and pMyr-Lamin served as positive and negative controls, respectively. *B*, GST pull-down assay showed that immobilized GST-γC but not GST alone interacted with Myc-tagged PYK2 and FAK in 293T cell lysates. Shown are anti-Myc Western blots detecting PYK2 or FAK proteins (*top two panels*) and Coomassie staining of input GST proteins (*middle*). To demonstrate the direct interaction, purified His-PYK2 was incubated with GST-γC, and the associated His-PYK2 was detected by anti-PYK2 Western blot. *C*, PYK2 is associated with full-length PCDH-γ in 293T cells. Different combinations of PYK2 and PCDH-γ expression plasmids were transfected into 293T cells. Anti-FLAG immunoprecipitation was performed to isolate PYK2-associated protein complex (*top*) or PCDH-γ complex (*bottom*). The input and immunoprecipitated proteins were detected by Western blots. Full-length C5 PCDH-γ isoform was used in the experiments, and the interactions were verified in IP from both directions. *D*, FAK interacts with the C5 isoform of PCDH-γ in 293T cells. Similar experiments except for FAK were performed as in *C*.

to 9E10 Myc-tagged PYK2 or FAK expressed in 293T cell lysates. Both Myc-tagged PYK2 and FAK interacted with GST-γC immobilized on glutathione-Sepharose beads but not with GST alone beads (Fig. 1*B*). To demonstrate that the interaction is direct, we tested whether the purified GST-γC protein can bind to a commercially available His-PYK2 purified from baculovirus-infected insect cells and detected a robust interaction between these two proteins (Fig. 1*B*, *bottom*). Unfortunately, the GST tag on an available recombinant FAK protein prevented us from performing a similar experiment on FAK.

To demonstrate the interaction between PCDH-γ and PYK2 in mammalian cells, 293T cells were transfected with FLAG epitope-tagged PYK2 and full-length PCDH-γ-C5, one of 22 PCDH-γ isoforms that have distinct extracellular domains but share a common γC. In the cells expressing both proteins, we found that PCDH-γ C5 was associated with PYK2 (Fig. 1*C*, *top*). We repeated a reciprocal experiment using FLAG-tagged PCDH-γ for immunoprecipitation (IP) and Myc-tagged PYK2 for Western blot, and the result confirmed that PCDH-γ interacted with PYK2 (Fig. 1*C*, *bottom*). In parallel, we performed co-IP experiments to determine the association of PCDH-γ with FAK. These experiments showed that PCDH-γ interacted with FAK in transfected 293T cells (Fig. 1*D*, *top* and *bottom*). Two other PCDH-γ isoforms, C4 and B2, were also found to interact with PYK2 and FAK (data not shown). Taken together, we conclude that PCDH-γ proteins can bind directly to both PYK2 and FAK through their common cytoplasmic domain.

PCDH-α Interacts with FAK and PYK2 in Vitro—Since different PCDH families contain distinct cytoplasmic domains, we asked whether interactions with PYK2 and FAK are specific to the PCDH-γ family. To test this possibility, we also determined whether PYK2 and FAK could be pulled down using GST fused to the cytoplasmic domain from PCDH-α (GST-αC). We did not include PCDH-β in the analysis, because individual PCDH-β isoforms have unique cytoplasmic domains. To our surprise, we found that both Myc-tagged PYK2 and FAK interacted with GST-αC in this assay (Fig. 2*A*).

In the CytoTrap two-hybrid system, we noticed that the interaction of pMyr-FAK with the bait pSOS-γC was relatively weak, whereas FAK interacted strongly with PCDH-γ in GST pull-down (Figs. 1*B* and 2*A*). One difference in these experiments is that pSOS-γC does not contain the last 10 lysine-rich amino acids. The shared cytoplasmic domain for PCDH-α (αC) contains an even longer lysine-rich tail. To evaluate whether the lysine-rich tails in both γC and αC contribute to the interactions among PCDH, PYK2, and FAK, we purified GST-γC-(1–115) and GST-αC-(1–119) lacking lysine-rich tails and examined their interactions with PYK2 and FAK using GST pull-down (Fig. 2*B*). This experiment demonstrated that the lysine tail in γC is important for binding of FAK but contributes less to the binding of PYK2 (Fig. 2*B*, *right panels*), providing an explanation for the weak interaction observed in the CytoTrap assay. The lysine tail in αC is not required for binding of either FAK or PYK2 (Fig. 2*B*, *left panels*).

To confirm the *in vitro* interaction between αC and PYK2 or FAK, we expressed the full-length C2, one of the PCDH-α isoforms, and FLAG-tagged PYK2 or FAK in 293T cells and used co-IP experiments to determine their biochemical interactions.

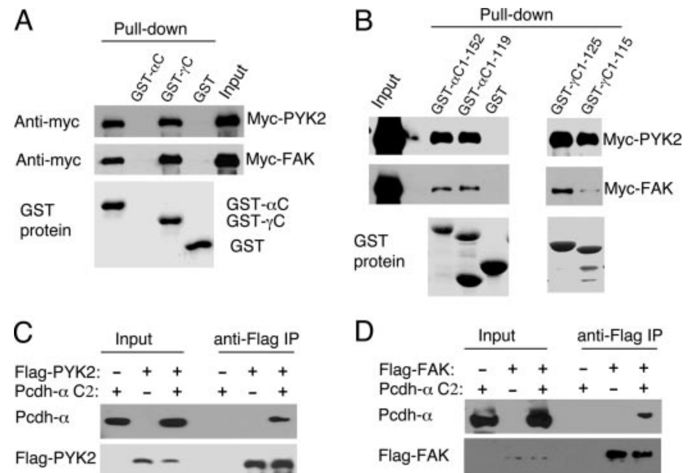

FIGURE 2. **PCDH-α interacts with PYK2 and FAK *in vitro*.** *A*, PYK2 and FAK interact with αC in the GST pull-down assay. Like GST-γC, GST-αC interacted with Myc-tagged PYK2 or FAK from 293T cell lysates. *B*, the lysine-rich tail of γC but not that of αC is required for binding to FAK. GST pull-down assays using αC-(1–152), αC-(1–119), γC-(1–125), and γC-(1–115) demonstrated that the last 10 amino acids in γC are important for the binding of FAK to PCDH-γ but have less effect on the binding to PYK2. *C* and *D*, PYK2 and FAK interact with full-length PCDH-α in 293T cells. FLAG-tagged PYK2 or FAK proteins were expressed with full-length C2 isoform of PCDH-α in 293T cells. Anti-FLAG IP and Western blots show PYK2 (*C*) or FAK (*D*) is associated with PCDH-α.

In both cases, PYK2 and FAK bound to PCDH-α C2 specifically (Fig. 2, *C* and *D*). Thus, our data have shown that PCDH-α can also interact with PYK2 and FAK *in vitro*.

PCDH-α, PCDH-γ, FAK, and PYK2 Are in Protein Complexes in Vivo—The fact that both PCDH-α and PCDH-γ directly bind PYK2 and FAK, combined with evidence that PCDH-α and PCDH-γ physically interact *in vivo* (29, 30), suggested the possibility that together these proteins form protein complexes *in vivo*. We first used co-IP experiments to confirm the association of PCDH-α and PCDH-γ in transfected 293T cells (Fig. 3*A*). PCDH-α and PCDH-γ are enriched in the membrane and even more in postsynaptic fractions from brain lysates. The affinity purification of PCDH from these fractions would be the most straightforward way to detect such protein complexes; our PCDH antibodies were, however, unsuitable for this application. For these experiments, we chose to affinity-purify PCDH-γ-containing complexes from brain lysates of a PCDH-γ-GFP knock-in mouse line (*Pcdh-γ^{fusg}* (16), in which a GFP cDNA is fused in-frame with the third constant exon of PCDH-γ. One advantage of this approach is that wild type mice would provide a negative control for co-IP using an anti-GFP antibody. Homozygous *Pcdh-γ$^{fusg/fusg}$* mice are grossly normal, and thus it is likely that the C-terminal GFP sequence does not interfere with the function of the cytoplasmic tail. To test this assumption, fusion proteins of two different PCDH-γ isoforms, PCDH-γ-C4-GFP (Fig. 3*B*) and PCDH-γ-B2-GFP (Fig. 3*C*), were tested for binding to FLAG-tagged FAK and PYK2 in transfected 293T cells. As shown in Fig. 3, *B* and *C*, GFP fusion at the C terminus of PCDH-γ did not interfere with PCDH-γ-FAK or PCDH-γ-PYK2 interaction. After validating our affinity purification strategy, we prepared total membrane fractions from *Pcdh-γ$^{+/fusg}$* mouse brain lysates at two different developmental stages (neonatal P0 and postnatal day 6 (P6)), affinity-

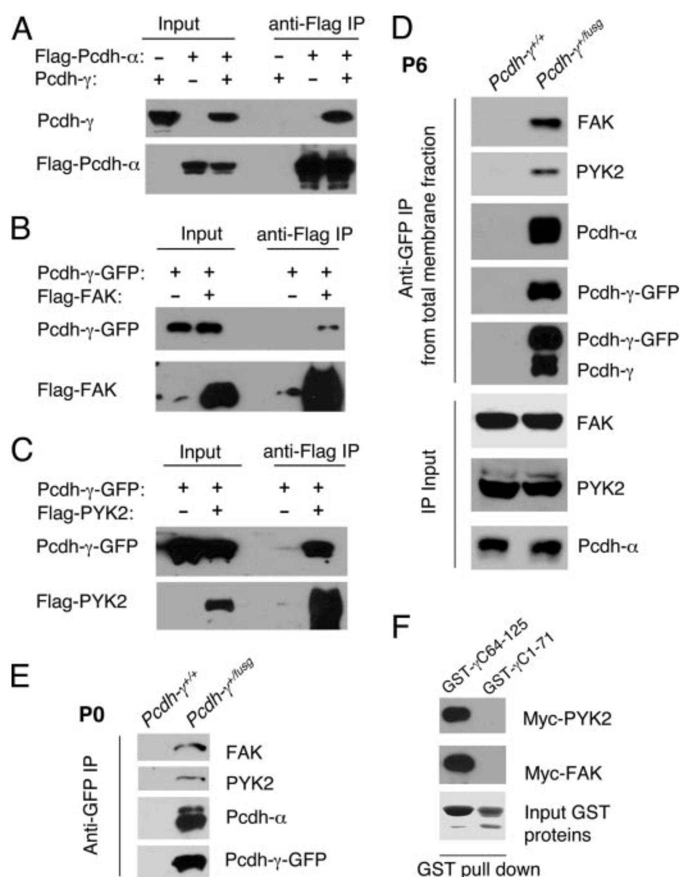

FIGURE 3. **PCDH-γ, PCDH-α, FAK, and/or PYK2 are in protein complexes in the brain.** *A*, PCDH-α and PCDH-γ are associated with each other in 293T cells. Anti-FLAG IP showed that FLAG-tagged PCDH-α bound to PCDH-γ in cells transfected with both expression vectors. *B* and *C*, FAK and PYK2 interact with PCDH-γ-GFP fusion proteins in transfected 293T cells. *D* and *E*, PCDH-γ protein complexes consist of multiple PCDH proteins and FAK or PYK2. PCDH-γ containing protein complexes were affinity-purified with anti-GFP beads using *Pcdh-γ*$^{+/fusg}$ brain tissues. The protein compositions of the complexes were analyzed by the indicated Western blots. P6 and P0 brain samples were used in *D* and *E*, respectively. *F*, PYK2 and FAK bind to the same C-terminal region in the shared cytoplasmic domain of PCDH-γ (amino acids 64–125). A GST pull-down assay using GSTγC-(1–71) and GSTγC-(64–125) is shown.

purified protein complexes with anti-GFP beads, and detected associated proteins by Western blot. Results in Fig. 3, *D* and *E*, illustrate that PCDH-α, PCDH-γ, FAK, and PYK2 co-immunoprecipitate with PCDH-γ-GFP. The choice of *Pcdh-γ*$^{+/fusg}$ heterozygous mice allows us to demonstrate that at least two different PCDH-γ molecules exist in a complex. This experiment, however, does not distinguish whether FAK and PYK2 are in the same PCDH-γ complex or in several separate complexes. The formation of PCDH-γ dimers or oligomers (Fig. 3*D*) in the cells makes it difficult to determine whether a single PCDH-γ molecule can bind to PYK2 and FAK simultaneously. Using the GST pull-down assay (Fig. 3*F*), we determined that both PYK2 and FAK interact with the same region within the shared cytoplasmic domain of PCDH-γ (the last 61 amino acids). This does not prove but suggests that PYK2 and FAK may compete for the same binding motif in a single PCDH-γ molecule. Nevertheless, PYK2 and FAK could still coexist in a large complex through bridges between PCDH-γ-PCDH-γ, PCDH-α-PCDH-α, and PCDH-α-PCDH-γ. In summary, the discovery of protein complexes that consist of PCDH-α, PCDH-γ, FAK, and/or PYK2 provides further evidence that α- and γ-protocadherins are associated with the two kinases *in vivo*.

PCDH-γ and PCDH-α Inhibit FAK and PYK2 Activity in Vitro—FAK and PYK2 function have been implicated in multiple cellular processes, including adhesion, migration, proliferation, and cell survival (31); thus, they are excellent candidates for downstream effectors of PCDH signaling. A central question is how interaction alters kinase or PCDH function. Presently, we consider four potential outcomes. First, PCDH could activate kinase activity, as in the case of intracellular association of integrin and FAK (32). Second, PCDH can negatively regulate the kinase activity of FAK and PYK2. Third, PCDH may be a substrate for PYK2 and FAK with phosphorylation of the cytoplasmic domain regulating PCDH function. Fourth, binding to PCDH may alter the subcellular localization of FAK and PYK2.

As a first step to examine the potential significance of PCDH-PYK2 and PCDH-FAK interactions, we mapped the domains of PYK2 and FAK that are required for interaction with PCDH-γ and PCDH-α, respectively. FAK and PYK2 share a similar domain structure that includes an N-terminal FERM domain, followed by a liner region, a tyrosine kinase catalytic domain, a proline-rich region, and a C-terminal FAT domain. To map the PCDH binding domains on FAK or PYK2, we expressed myristoylated full-length and truncated PYK2 or FAK proteins in the reporter yeast strain and compared their interactions with the bait (Fig. 4*A*). This experiment showed that γC interacted with the kinase domain of PYK2 (Fig. 4*A*, *left*). No further mapping was done for FAK, because the interaction was weak (Fig. 4*A*, *right*). Furthermore, we used an independent approach-GST pull-down to verify this result. We compared interactions of immobilized GST-γC and GST-αC with expressed full-length and truncated FAK or PYK2 in 293T cell lysates (Fig. 4, *B* and *C*). Both γC and αC bound strongly to N-terminal truncated FAK and PYK2 (*lane 6* in Fig. 4, *B* and *C*). Robust interactions with FAK kinase domain (Fig. 4*B*, *lane 7*) and weak interactions with PYK2 kinase domain were also detected for γC (Fig. 4*C*, *lane 7*).

Interaction of the PCDH cytoplasmic domain with the kinase domain of FAK and PYK2 is consistent with the possibility that γC and αC are substrates for PYK2 and FAK. Therefore, we tested this possibility using an *in vitro* kinase assay with recombinant FAK and PYK2. Neither GST-γC nor GST-αC was phosphorylated in these assays, although both FAK and PYK2 displayed strong kinase activity toward the cytoplasmic domain of N-cadherin (Fig. 4*D*) and a commonly used FAK/PYK2 substrate, E4Y1 (poly(Glu)/poly(Tyr) ratio of 4:1) polypeptides (data not shown) (see below). Thus, γC and αC are not a substrate for these kinases *in vitro*.

Next, we tested the possibility that γC and αC could function as negative regulators of the kinase activity. FLAG-tagged FAK or PYK2 was expressed in 293T cells and purified by anti-FLAG IP. The purified kinases were subjected to *in vitro* kinase assays using the E4Y1 polypeptide as an exogenous phosphorylation substrate in the presence of different amounts of purified GST or GST fusion proteins (24). Purified FAK and PYK2 phosphorylate E4Y1 polypeptides as well as undergo autophosphoryla-

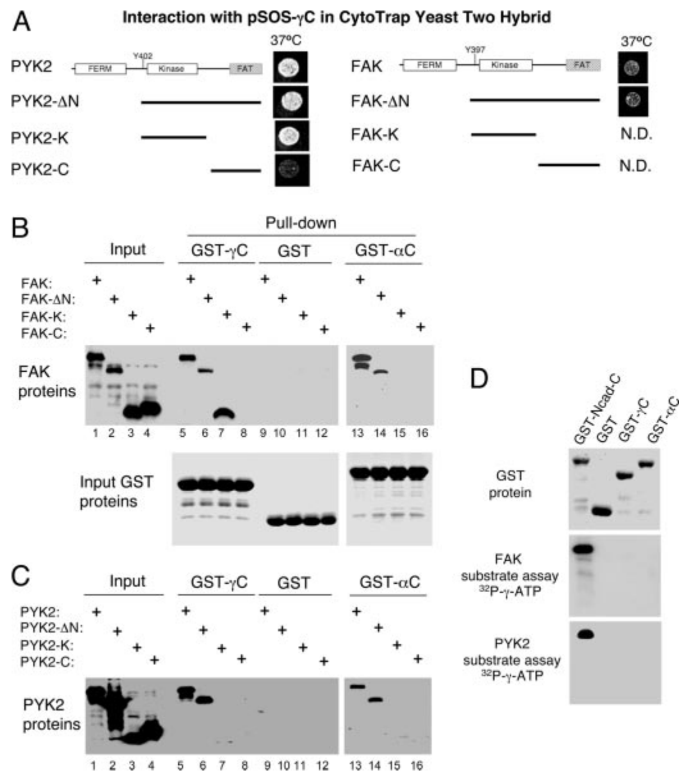

FIGURE 4. **Mapping the interaction domains in FAK and PYK2 with PCDH-γ and PCDH-α.** *A*, schematic drawings of domain organization of the wild type and deletion mutant PYK2 or FAK. The yeast growth at 37 °C indicates an interaction between different PYK2 and FAK protein with the bait pSOS-γC, demonstrating that the kinase domain of PYK2 interacts with γC. The relatively weak interaction of FAK with γC precluded further domain mapping. *B* and *C*, interactions between GSTγC and GSTαC with FAK (*B*) or PYK2 (*C*) deletion mutant proteins. The purified GSTγC and GSTαC were used to incubate with the cell lysates expressing different FAK or PYK2 deletion mutant proteins. GST pull-down assays show that γC interacts with the kinase domain in FAK (*lane 7* in *B*) or PYK2 (*lane 7*, a weak band in *C*), and αC interacts with a region that contains both kinase and FAT domains (*lane 14* in *B* and *C*). *D*, the cytoplasmic domains of PCDH-α and PCDH-γ are not substrates for FAK and PYK2 *in vitro*. *In vitro* kinase assays were carried out using purified recombinant FAK and PYK2 (100 ng/reaction). GST-γC and GST-αC (10 μg/reaction) were tested as their substrates. GST-N-Cad-C and GST alone served as positive and negative controls, respectively. Shown are the Coomassie staining of input substrate proteins and radioautography of [γ-^{32}P]ATP kinase assays. *N.D.*, not determined.

tion (Fig. 5). In the following experiments, we used both analytical methods to determine relative kinase activity. In these studies, both GST-αC and GSY-γC inhibited the kinase activity of FAK and PYK2 in a dose-dependent manner, whereas GST alone had little effect (Fig. 5, *A* and *B*). Since FAK and PYK2 are known to bind Src family kinases, it is therefore possible that GST-αC and GST-γC inhibit E4Y1 phosphorylation by affecting Src kinase activity associated with FAK or PYK2. To rule out this possibility, we repeated the experiments using PYK2 and FAK expressed from SYF fibroblast cells that are deficient for all three Src family kinases (33), and we observed a similar inhibitory effect on PYK2 and FAK activity (Fig. 5*C*). Taken together, our results indicate that PCDH-α and PCDH-γ function as negative regulators of FAK and PYK2.

The model for FAK and PYK2 activation consists of sequential steps of tyrosine phosphorylation (34). Autophosphorylation of Tyr^{397} within the linker region of FAK represents the first step of kinase activation, and the subsequent conformational change creates a docking site for Src family kinases and further activation. The inhibitory effects of GST-γC and GST-αC *in vitro* are relatively modest. This is in part due to the fact that FAK and PYK2 purified from overexpressed cells are already partially active as evidenced by the Tyr(P)^{397} and Tyr(P)^{402} Western blots (35) (data not shown) (Fig. 6*E*). It has been recently shown that the N-terminal FERM domain of FAK plays an autoinhibitory role for the initial step of FAK activation (35). We speculate that the cytoplasmic domains of PCDH-γ and PCDH-α might have an analogous inhibitory function at the first step of kinase activation.

Cofractination of PCDH-γ and PCDH-α with FAK and PYK2—In vitro biochemical analysis suggested a possible mode of action, inhibition of PYK2 and FAK by protocadherins. If so, PYK2 and FAK associated with PCDH should have reduced activity relative to unbound protein. To test this hypothesis, we first used cell fractionation to examine the subcellular distribution of PCDH-γ, PYK2, and FAK. Fig. 6*A* shows that PYK2 and FAK are present in soluble cytosolic fraction (S2), membrane fractions (P2 and Syn), and detergent-resistant PSD fraction. By contrast, PCDH-γ is enriched in the membrane fractions, most noticeably in the PSD (16). Consistent with these results, we found that PYK2 and FAK immunoreactivity largely overlaps with PCDH-γ-GFP in the dendrites (PSD95-positive) of mature hippocampal neurons (Fig. 6*B*). Therefore, we chose to analyze the effect of PCDH association on FAK and PYK2 activity in enriched membrane preparations. We used phospho-specific antibodies that recognize Tyr(P)^{397} on FAK and Tyr(P)^{402} on PYK2 as a surrogate for kinase activity, since these autophosphorylation events are essential for *in vivo* activation of FAK and PYK2, respectively (36, 37). As shown in Fig. 6*C*, although similar amounts of total FAK and PYK2 were used for comparison, the Tyr(P)^{397} signals on FAK and the Tyr(P)^{402} signals on of PYK2 were significantly decreased in the membrane fraction. This is consistent with our model that PCDH proteins inhibit FAK and PYK2 *in vivo*. To further test this observation, we performed sucrose gradient ultracentrifugation analysis on the distribution of FAK, Tyr(P)^{397}-FAK, PYK2, Tyr(P)^{402}-PYK2, and PCDH proteins from total brain membrane proteins solubilized in Triton X-100 (Fig. 6*D*). Several controls, including synaptic vesicle protein, synapsin I, classic cadherins, adhesion molecule NCAM, and neurofilament protein NF200, were used to profile sucrose gradient fractions. As shown in Fig. 6*D*, although the distribution of PCDH-γ and PCDH-α largely overlaps with that of PYK2 in sucrose gradient fractions (fractions 4–8), Tyr(P)^{402}-PYK2 (activated form) is most abundant in fractions (fractions 3 and 4) and has no or little overlap with PCDH-γ. This result suggests that the PYK2 associated with PCDH-γ and possibly with PCDH-α is most likely in a non-phosphorylated and inactive form. Our sucrose gradient analysis also shows that the distributions of PCDH-γ and PCDH-α overlap, and both peak in higher density fractions (fractions 6 and 7 for PCDH-γ and fractions 5–7 for PCDH-α), which has an estimated size of 600 kDa, in comparison with other membrane proteins, such as NCAM and cadherins (fractions 3–5). The described protein distribution profiles in the sucrose gradient analyses were highly reproducible in six independent ultracentrifugation experiments. Because we have found that

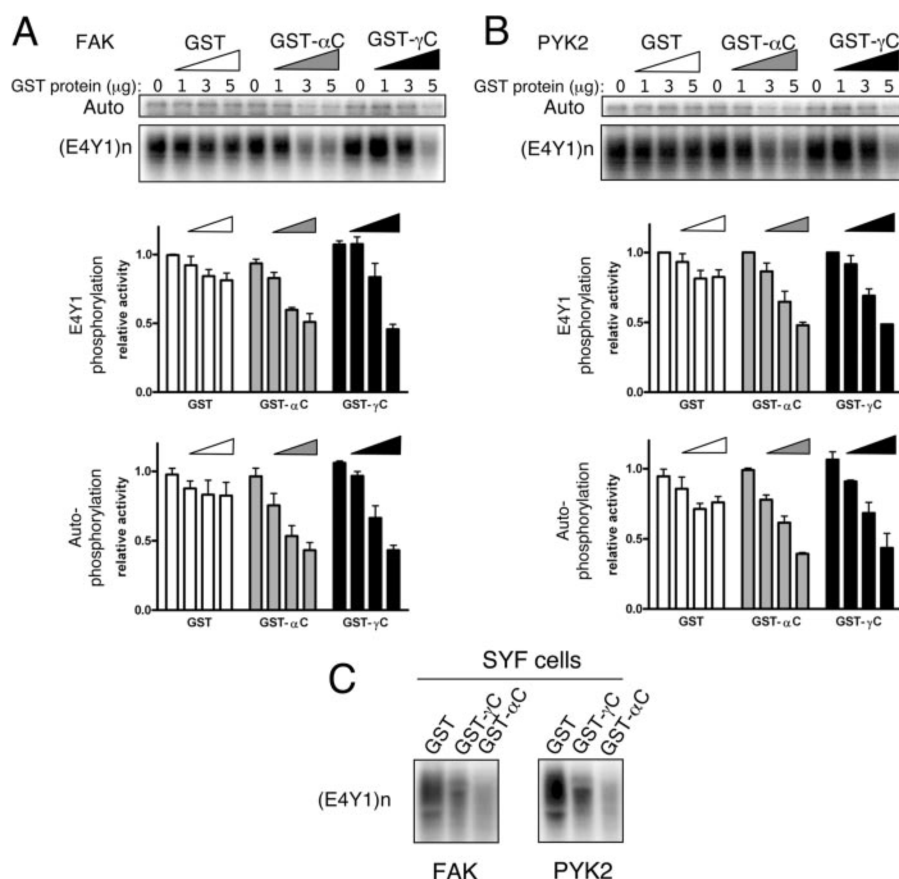

FIGURE 5. **γC and αC inhibit FAK and PYK2 kinase activity *in vitro*.** *A* and *B*, FLAG-tagged FAK (*A*) or PYK2 (*B*) were immunoprecipitated from 293T cell lysates. Identical aliquots of the purified kinases were assayed for their activity using E4Y1 (10 μg/reaction) as an exogenous substrate in the presence of increasing amounts of purified GST, GST-γC, and GST-αC, as indicated. The relative levels of E4Y1 phosphorylation as well as autophosphorylation of FAK or PYK2 were measured using a PhosphorImager. Relative kinase activity was normalized to kinase activity without any GST proteins. The means and S.E. of the relative kinase activities from three independent assays are shown. Data were analyzed using two-way analysis of variance (protein × dosage). $p < 0.03$. *C*, the effect of γC and αC on the kinase activity of FAK or PYK2 isolated from SYF cells. Shown are PhosphorImager acquired images of E4Y1 phosphorylation by FAK or PYK2. 5 μg of indicated GST fusion proteins were used in the kinase assay.

FAK and PCDH overlap to a lesser extent and, more importantly, we could not separate the distribution of total FAK protein from that of Tyr(P)^{397}-FAK, we could not make a definitive conclusion on the autophosphorylation status of FAK that is cofractionated with PCDH. Despite the caveat, our analysis provides correlative evidence that PCDH-γ and PCDH-α are inhibitory to PYK2 activity *in vivo*.

PCDH-γ and PCDH-α Inhibit FAK and PYK2 Activity in Vivo—The fractionation and sucrose gradient experiments suggest that PYK2 and FAK are probably inactive when bound to PCDH but do not prove this model. To directly test whether PCDH inhibits PYK2 and FAK in the brain, we compared autophosphorylation levels of PCDH-associated PYK2 and FAK with those from the total brain lysates. We used anti-GFP co-IP to purify PCDH-associated FAK or PYK2 from *Pcdh-γ$^{+/fusg}$* brain lysates, as described above. When an equal amount of PYK2 proteins from IP or brain lysates was loaded for Western blot, we detected robust Tyr(P)^{402} signals from the brain lysates and very little from the IP sample (Fig. 7*A*), demonstrating that PCDH-associated PYK2 is inactive. Similar comparison of Tyr(P)^{397} on FAK demonstrates that PCDH-associated FAK is inactive as well (Fig. 7*B*). Therefore, we conclude that the activity of both PYK2 and FAK is inhibited when bound to PCDH-γ and/or PCDH-α *in vivo*.

If the inhibitory effect of PCDH on PYK2 or FAK is biologically significant, we predicted that the membrane-bound PYK2 and/or FAK activity would increase in *Pcdh-γ$^{del/del}$* mice or in mice lacking both *Pcdh-α* and *Pcdh-γ*. Currently, a double knock-out for *Pcdh-α* and *Pcdh-γ* mouse strain is not available. Therefore, we tested our prediction in *Pcdh-γ$^{del/del}$* mice. Brains from *Pcdh-γ$^{del/del}$* and *Pcdh-γ$^{+/+}$* neonates were harvested to produce total membrane proteins. Equivalent amounts of total membrane proteins from both genotypes were loaded onto a sucrose gradient for ultracentrifugation. Equal amounts of proteins in corresponding fractions from different genotypes were used for Western blot analysis to compare the abundance and distribution of proteins of interest. As expected, PCDH-γ proteins were completely absent in *Pcdh-γ$^{del/del}$* samples (Fig. 7*C*, *right*), whereas PCDH-α, cadherins, and tubulin remained constant (Fig. 7*C*, *bottom three panels*), serving as internal controls for normalized loading for each sucrose fractions. Deletion of all PCDH-γ did not appear to have a significant effect on the distribution or activity of FAK. Most noticeably, in *Pcdh-γ$^{del/del}$* fractions, Tyr(P)^{402}-PYK2 was significantly increased, although the PYK2 protein level might be slightly lower than that of the control (Fig. 7*C*, *top two panels*). Thus, PCDH-γ is required for repressing PYK2 activity *in vivo*.

Given the fact that both PCDH-α and PCDH-γ are capable of inhibiting PYK2 activity *in vitro* (Fig. 5), it is intriguing to note that the remaining PCDH-α proteins does not compensate for the loss of PCDH-γ. This observation might reflect the fact that PCDH-γ transcripts are expressed at a level 4 times higher that that of PCDH-α in the mouse brain. Alternatively, this might result from different effects of α- and γ-protocadherins on downstream signal transduction pathways. *Pcdh-α$^{-/-}$* mice are viable, and *Pcdh-γ$^{del/del}$* are neonatal lethal (16, 20). Although functional compensation could play a role, PCDH-γ appears to be essential and unique at least in some aspects. The phospho-specific antibodies are not suitable for immune staining on the tissue samples and thus prevent us from analyzing cell populations with up-regulated PYK2 activity. We could not exclude the possibility that FAK activity was altered at different devel-

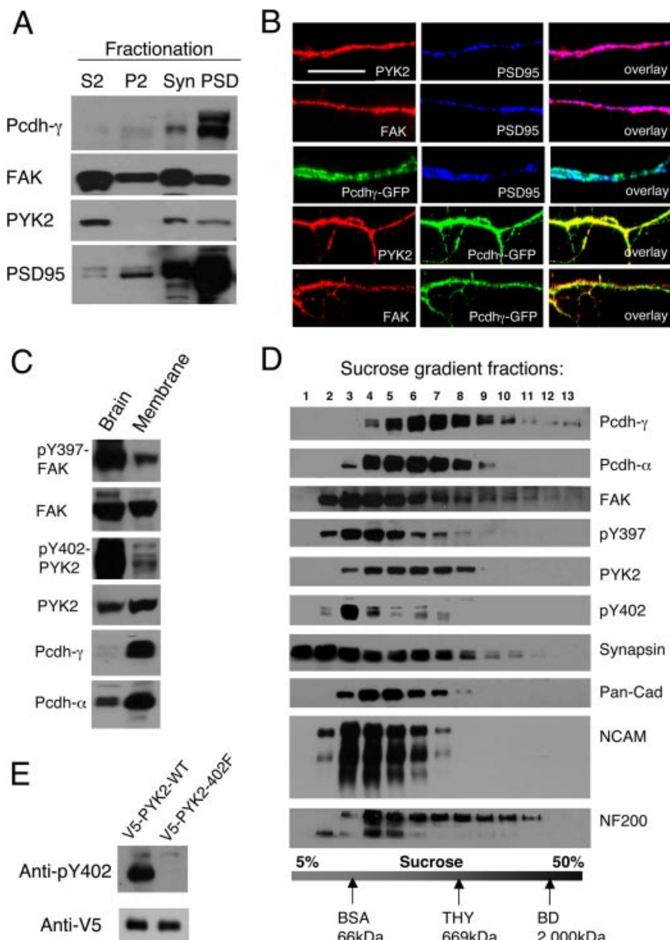

FIGURE 6. **Cofractionation of PYK2 and FAK with PCDH.** *A*, subcellular fractionation of brain lysates shows that FAK and PYK2 are present in the soluble cytosolic fraction (S2), membrane fractions (P2 and Syn), and PSD, whereas PCDH-γ is present in the membrane fraction and concentrated in the PSD. *B*, PCDH-γ-GFP proteins are overlapped with FAK and PYK2 in the dendrites of *Pcdh-γ^fusg^* hippocampal neuron culture. Dendrites are identified by PSD95 staining. *Bar*, 20 μm. *C*, comparison of phosphorylation levels on Tyr(P)^{397} on FAK and Tyr(P)^{402} on PYK2 in the whole brain and total membrane samples indicates that membrane-bound FAK and PYK2 have lower kinase activity. Shown are panels of Western blots that compare levels of FAK, Tyr(P)^{397}, PYK2, Tyr(P)^{402}, PCDH-γ, and PCDH-α. Note that multiple bands of Tyr(P)^{402}-PYK2 were detected in the membrane fractions that might reflect multiple phosphorylation events of PYK2. *D*, sucrose gradient ultracentrifugation analysis of total membrane proteins shows that Tyr(P)^{402}-PYK2 is absent in the fractions that have significant overlap with PCDH proteins, whereas Tyr(P)^{397}-FAK and FAK cofractionate. Shown are Western blots analyzing the abundance and distribution of indicated protein in 5–50% sucrose gradient fractions. The size markers for the sucrose gradient ultracentrifugation are bovine serum albumin (*BSA*; 66 kDa), thyroglobulin (*THY*; 669 kDa), and blue detran (*BD*; 2,000 kDa). *E*, the specificity of Tyr(P)^{402}-PYK2 antibody is confirmed by Western blots of V5-tagged wild type PYK2 and Y402F PYK2 proteins overexpressed in 293T cells. *pY*, Tyr(P).

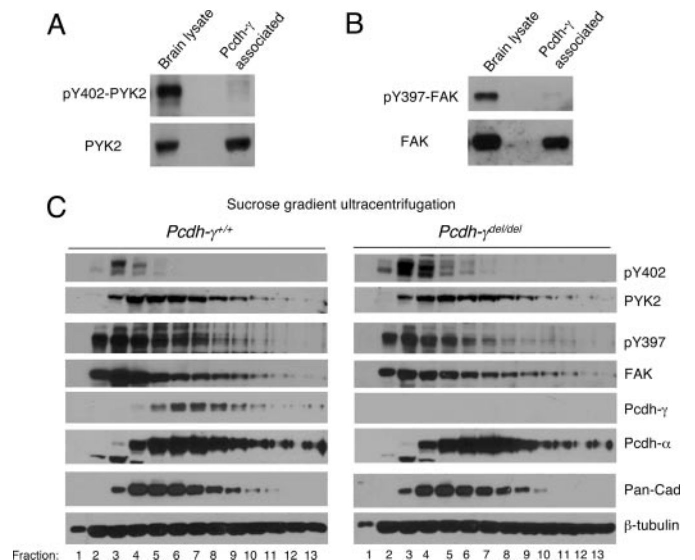

FIGURE 7. **PCDH-γ and PCDH-α inhibit PYK2 and FAK activity in the brain.** *A* and *B*, inactive PYK2 and FAK are associated with PCDH protein complex in the brain. Shown are comparisons of PYK2 and Tyr(P)^{402}-PYK2 levels from *Pcdh-γ^+/fusg^* total brain lysates and affinity-purified PCDH-γ protein complex with anti-GFP antibody (*A*). FAK and Tyr(P)^{397}-FAK are shown in *B*. *C*, PYK2 is abnormally activated in *Pcdh-γ^del/del^* mice. Similar amounts of total brain membrane proteins from both wild type and *Pcdh-γ^del/del^* neonates were subjected to sucrose gradient ultracentrifugation and Western blot analyses. Each pair of Western blots from two genotypes was obtained with equal amounts of proteins in corresponded fractions and was probed and developed simultaneously. The abundance and distribution of PCDH-α, cadherins, and β-tubulin were almost identical, and they served as the internal controls for the experimental procedures. Tyr(P)^{402}-PYK2 intensity was significantly up-regulated in the absence of PCDH-γ, whereas PYK2 protein level slightly decreased and the distribution remained the same in the mutants. Both FAK and Tyr(P)^{397}-FAK levels were not significantly changed in *Pcdh-γ^del/del^* mice. *pY*, Tyr(P).

opment stages or in different subpopulations of neurons. Nevertheless, our data have demonstrated that PCDH-γ plays a significant role in the negative regulation of PYK2 in the brain.

Overexpression of PYK2 Induces Apoptosis in the Chicken Spinal Cord—Genetic deletion of PCDH-γ in mice and morpholino-mediated inhibition of PCDH-α in zebrafish induce neuronal apoptosis in the central nervous system (16, 38). It was reported that expression of wild type but not a kinase-dead PYK2 induces apoptosis in fibroblast and epithelial cells, suggesting a role for PYK2 in the regulation of apoptosis under certain conditions (39). To examine the possibility that the abnormal up-regulation of PYK2 activity contributes to the apoptotic phenotype, we overexpressed PYK2 in the developing chicken spinal cord by *in ovo* electroporation (27). At stage 12, we injected and electroporated expression plasmids into one side of the spinal cord at the thoracic level. Using this approach, we first asked whether PYK2 exhibits an effect on cell proliferation. 24 or 72 h after electroporation, labeling of M-phase cells using anti-phospho-H3 antibody showed that the numbers of phospho-H3-positive progenitors (labeled in *green*) were comparable between the PYK2 expressing cells (labeled in *red*) and the nonelectroporated cells (unlabeled in the red channel) (Fig. 8*A*). Similarly, pulse labeling of S-phase cells with BrdUrd confirmed that overexpression of PYK2 has no significant effect on cell proliferation in the spinal cord (Fig. 8*B*).

Finally, we tested whether overexpression of wild type PYK2 could induce apoptosis in the chicken spinal neurons. After electroporating different expression vectors, apoptotic neurons were detected by a cleaved caspase-3 antibody staining (Fig. 8, *C* and *D*). Quantitative analysis of apoptotic cells showed that overexpression of wild type PYK2 induced a statistically significant increase of spinal neuronal apoptosis compared with the LacZ-negative control (Fig. 8*E*). Introduction of kinase-dead PYK2 showed no significant increase of apoptosis, as suggested by the previous study in nonneuronal cells (39). Overexpression of either wild type or kinase-dead FAK did not alter levels of

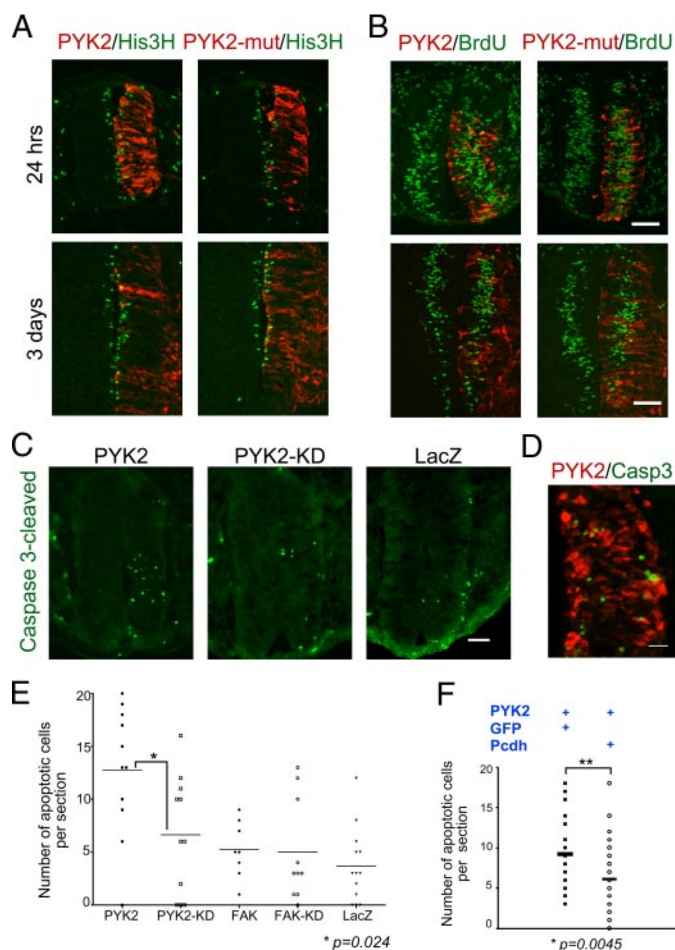

FIGURE 8. **PYK2 overexpression induces apoptosis in the developing chicken spinal cord.** *A* and *B*, overexpression PYK2 has no effect on cell proliferation in the chicken spinal cord. *A*, V5-tagged wild type and kinase-dead (*KD*) PYK2 were overexpressed in the right side of the spinal cord by electroporation at stage 12. Anti-phosphohistone H3 labeling (*green cells* on *both sides* of the central canal) shows that both electroporated (*red*) and nonelectroporated (*dark*) sides have similar numbers of mitotic cells 24 or 72 h after electroporation. *B*, BrdUrd administration to label S-phase proliferating cells shows that introduction of either wild type or kinase-dead PYK2 has little effect on BrdUrd incorporation. Note that in both *A* and *B*, V5-PYK2 is mostly localized in the neuronal processes, and phospho-H3 or BrdUrd labeling is exclusively in the nucleus. No apparent overlap of both signals was observed. *C–E*, overexpression of wild type but not kinase-dead PYK2 induces apoptosis in the spinal cord. *C*, representative images of anti-cleaved caspase-3 staining of chicken spinal cord sections that were electroporated with the indicated expression vectors. V5-tagged LacZ was used as a negative control. Embryos were harvested 24 h after electroporation. A small number of apoptotic cells were observed in the control sections due to the electroporation procedure. *D*, double-labeling of PYK2 (anti-V5; *red*) and active caspase-3 (*green*) shows that many caspase-3-positive nuclei were close to V5-stained soma or neuronal processes, suggesting that the apoptotic effect of PYK2 is probably cell-autonomous. *E*, quantitative analysis of the apoptotic cells in the PYK2 overexpressing spinal cord. Active caspase-3-positive cells were counted on sections from individual embryos. In the graph, the average number of active caspase-3-positive cells per section from individual embryos is plotted for each protein expressed. The results were subjected to *t* test and a *p* value of 0.024 was obtained between wild type and kinase-dead PYK2 samples. *F*, overexpression of PCDH-γ attenuates the apoptosis-inducing activity of PYK2. PCDH-γ and PYK2 expression vectors (at a ratio of 3:1) were electroporated into the chicken neural tubes as in *C*. A GFP expression vector was used as a negative control. The number of apoptotic cells was decreased upon co-expression of PYK2 with PCDH-γ, suggesting that PCDH-γ inhibits the activity of PYK2. The data were analyzed as in *E*. *Bars*, 50 μm in *A–C* and 20 μm in *D*.

apoptosis (Fig. 8*E*). All FAK or PYK2 proteins used in the experiment are expressed at a comparable level in transfected cells, suggesting that the absence of phenotype in mutant PYK2- or FAK-expressing spinal cords is not due to lower expression levels of these proteins (data not shown). Therefore, up-regulation of PYK2 activity is specific for the observed apoptotic phenotype. To test whether overexpression of PCDH-γ is capable of inhibiting apoptotic activity of PYK2, we co-expressed PCDH-γ and PYK2 in the chicken spinal cord and found that PCDH-γ overexpression attenuated PYK2 activity in this assay (Fig. 8*F*). These results, together with the finding that membrane-bound PYK2 activity is increased in *Pcdh-*$\gamma^{del/del}$ mice, demonstrate that PCDH-mediated inhibition of proapoptotic activity of PYK2 may have a role in the regulation of neuronal survival.

DISCUSSION

The α- and γ-families of protocadherins have been implicated in the regulation of neuronal survival and synaptic connectivity in genetic model systems, including mouse and zebrafish (16, 38). In this study, we have identified the first set of downstream signaling molecules for PCDH molecules. Both α- and γ-PCDH proteins bind to PYK2 and FAK, through their distinct cytoplasmic domains. Upon forming complexes with PYK2 or FAK, PCDH inhibits its kinase activity. Genetic deletion of *Pcdh-*γ in mice leads to an abnormal increase of PYK2 activity in neurons and overexpression of PYK2 increases neuronal death in the spinal cord. These results are consistent with a model in which PCDH-γ and PCDH-α form protein complexes that repress the activity of PYK2. Abnormal activation of PYK2 might contribute to the excessive apoptosis observed in *Pcdh-*$\gamma^{del/del}$ mice. The identification of PCDH downstream effectors provides an entry point to unveil the signaling pathways linking protocadherins to neuronal survival and connectivity.

FAK and PYK2 are two closed related nonreceptor cytoplasmic tyrosine kinases. FAK is activated by integrin engagement and is essential for the dynamic turnover of focal adhesions in cells (32). In contrast, PYK2 is only weakly activated by integrins, but it is robustly induced by a different set of stimuli, such as Ca^{2+} signaling, protein kinase C, and G-protein-coupled receptors. Active FAK or PYK2 recruits Src to form a dual kinase complex that functions in the regulation of a number of signaling events, including the Rho-GTPase, mitogen-activated protein kinase, and phosphatidylinositol 3-kinase-Akt pathways (31). PYK2 is abundantly expressed in the brain and important for neuronal functions (40). PYK2 activation has been shown to induce apoptosis in nonneuronal cells, such as fibroblasts and epithelial cells (39). The N-terminal FERM domain and tyrosine kinase activity of PYK2 are required for its apoptotic activity. It has also been shown that FIB200, a negative regulator of PYK2, is capable of attenuating the death-inducing activity of PYK2 (24). *Pcdh-*$\gamma^{del/del}$ mice have a significant increase of neuronal death and degeneration in the central nervous system (16). Similarly, inhibition of PCDH-α using morpholinos in zebrafish results in widespread neuronal apoptosis (38). In this report, we have provided evidence that PCDH-α and PCDH-γ negatively regulate PYK2 activity, and PYK2 activity is abnormally up-regulated upon depletion of PCDH-γ. Therefore, we have proven that PCDH functions as a negative regulator of PYK2 activity *in vivo*. Moreover, overex-

pression of wild type PYK2 but not kinase-dead PYK2 induced neuronal death in the developing chicken spinal cord, recapitulating some aspects of apoptotic phenotype observed in mice and zebrafish. In addition, PYK2 activation under some pathological conditions, such as ischemia or convulsions, has also been found in the central nervous system (41, 42). Taken together, these studies suggest that up-regulation of PYK2 activity could be one of the mechanisms that contribute to the programmed or excitatory neuronal death during development and in diseases. The presented results are consistent with but do not prove that PYK2 activation is essential for the induction of apoptosis in *Pcdh-*$\gamma^{del/del}$ mice. It has been reported that *PYK2*$^{-/-}$ mice are grossly normal but exhibit signaling defects in macrophages and osteoclasts (43–45). It becomes crucial to examine whether neuronal apoptosis is affected in *Pcdh-*$\gamma^{del/del}$; *PYK2*$^{-/-}$ mice in the future.

FAK activity appeared unchanged in our analysis of *Pcdh-*$\gamma^{del/del}$ mice. One explanation could be the presence of related PCDH-α in the protein complexes (29). As seen in the *in vitro* kinase assays, αC efficiently inhibits the activity of FAK and PYK2. All four proteins might form a large membrane complex in the brain. Thus, PCDH-α and PCDH-γ could share functional redundancy. The interdependence of PCDH-α and PCDH-γ was first proposed as an intracellular trafficking mechanism for PCDH-α proteins (29). However, more recent evidence has shown that surface delivery of either α- or γ-PCDH is independent from each other (30). Here we demonstrated that α- and γ-PCDH share common downstream effectors and exhibit similar biochemical properties in regulating PYK2 and FAK activity. Thus, functional redundancy might exist in the PCDH downstream signaling pathways. This notion of redundancy is also supported by the observation that the apoptosis and synaptic deficits are only in subpopulations of neurons, most noticeably in the interneurons of spinal cord and some regions of the brain (16). Certain subsets of neurons (*e.g.* spinal motoneurons) are obviously unaffected by PCDH-γ deficiency. A similar observation has been made in the PCDH-α morpholino-injected zebrafish. Although neuronal apoptosis is found throughout the central nervous system, subsets of spinal sensory or motor neurons examined in the study are not affected (38). The lack of general effect in loss-of-function PCDH-α or -γ mutant animals could be due to compensation by other related PCDH (3). Interestingly, mice with a null mutation of PCDH-α have a less dramatic phenotype. PCDH-α mutant mice are viable and fertile but exhibit abnormality in axon convergence of olfactory sensory neurons (20). It is interesting to note that different vertebrate species have differential requirements for PCDH molecules. Despite the suggestive evidence, a definitive answer to the question of protocadherin redundancy will certainly benefit from constructing mice deficient for all PCDH gene clusters.

If indeed PCDH-α and PCDH-γ play an inhibitory role in regulating FAK activity *in vivo*, an increase in FAK activity could account for some phenotypical changes observed in *Pcdh* mutants, including synaptic loss as well as the axonal targeting defect. FAK is required for netrin signaling and responsible for axon outgrowth and guidance, including spinal commissural axons (46–49). Inhibition of PCDH-α function in zebrafish led to a significant reduction of spinal commissural axons (38). FAK also plays a role in the control axonal branching and synapse formation in Purkinje cells as well as hippocampal neurons (50). These data, together with the findings that PCDH-γ plays a role in certain aspects of synaptic development and that PCDH-α is involved in axon targeting (19, 20), make it tempting to consider FAK an attractive candidate to mediate PCDH signals downstream. It is possible that functional redundancy among many PCDH molecules prevents us from unveiling the regulation of FAK *in vivo*. Future experiments to further reduce the protocadherin diversity are necessary to address this question directly.

Acknowledgments—We thank Dr. William Klein for advice on hippocampal neuron culture and Drs. Robert Holmgren and Andy Dudley for critical reading and advice on the manuscript.

REFERENCES

1. Takeichi, M. (1995) *Curr. Opin. Cell Biol.* **7,** 619–627
2. Yagi, T., and Takeichi, M. (2000) *Genes Dev.* **14,** 1169–1180
3. Halbleib, J. M., and Nelson, W. J. (2006) *Genes Dev.* **20,** 3199–3214
4. Wu, Q., and Maniatis, T. (1999) *Cell* **97,** 779–790
5. Noonan, J. P., Grimwood, J., Schmutz, J., Dickson, M., and Myers, R. M. (2004) *Genome Res.* **14,** 354–366
6. Wu, Q. (2005) *Genetics* **169,** 2179–2188
7. Kohmura, N., Senzaki, K., Hamada, S., Kai, N., Yasuda, R., Watanabe, M., Ishii, H., Yasuda, M., Mishina, M., and Yagi, T. (1998) *Neuron* **20,** 1137–1151
8. Frank, M., Ebert, M., Shan, W., Phillips, G. R., Arndt, K., Colman, D. R., and Kemler, R. (2005) *Mol. Cell Neurosci.* **29,** 603–616
9. Zou, C., Huang, W., Ying, G., and Wu, Q. (2007) *Neuroscience* **144,** 579–603
10. Wang, X., Su, H., and Bradley, A. (2002) *Genes Dev.* **16,** 1890–1905
11. Tasic, B., Nabholz, C. E., Baldwin, K. K., Kim, Y., Rueckert, E. H., Ribich, S. A., Cramer, P., Wu, Q., Axel, R., and Maniatis, T. (2002) *Mol. Cell* **10,** 21–33
12. Esumi, S., Kakazu, N., Taguchi, Y., Hirayama, T., Sasaki, A., Hirabayashi, T., Koide, T., Kitsukawa, T., Hamada, S., and Yagi, T. (2005) *Nat. Genet.* **37,** 171–176
13. Kaneko, R., Kato, H., Kawamura, Y., Esumi, S., Hirayama, T., Hirabayashi, T., and Yagi, T. (2006) *J. Biol. Chem.* **281,** 30551–30560
14. Ribich, S., Tasic, B., and Maniatis, T. (2006) *Proc. Natl. Acad. Sci. U. S. A.* **103,** 19719–19724
15. Obata, S., Sago, H., Mori, N., Rochelle, J. M., Seldin, M. F., Davidson, M., St. John, T., Taketani, S., and Suzuki, S. T. (1995) *J. Cell Sci.* **108,** 3765–3773
16. Wang, X., Weiner, J. A., Levi, S., Craig, A. M., Bradley, A., and Sanes, J. R. (2002) *Neuron* **36,** 843–854
17. Phillips, G. R., Huang, J. K., Wang, Y., Tanaka, H., Shapiro, L., Zhang, W., Shan, W. S., Arndt, K., Frank, M., Gordon, R. E., Gawinowicz, M. A., Zhao, Y., and Colman, D. R. (2001) *Neuron* **32,** 63–77
18. Phillips, G. R., Tanaka, H., Frank, M., Elste, A., Fidler, L., Benson, D. L., and Colman, D. R. (2003) *J. Neurosci.* **23,** 5096–5104
19. Weiner, J. A., Wang, X., Tapia, J. C., and Sanes, J. R. (2005) *Proc. Natl. Acad. Sci. U. S. A.* **102,** 8–14
20. Hasegawa, S., Hamada, S., Kumode, Y., Esumi, S., Katori, S., Fukuda, E., Uchiyama, Y., Hirabayashi, T., Mombaerts, P., and Yagi, T. (2008) *Mol. Cell Neurosci.* **38,** 66–79
21. Haas, I. G., Frank, M., Veron, N., and Kemler, R. (2005) *J. Biol. Chem.* **280,** 9313–9319
22. Hambsch, B., Grinevich, V., Seeburg, P. H., and Schwarz, M. K. (2005) *J. Biol. Chem.* **280,** 15888–15897
23. Aronheim, A., Zandi, E., Hennemann, H., Elledge, S. J., and Karin, M. (1997) *Mol. Cell. Biol.* **17,** 3094–3102

24. Ueda, H., Abbi, S., Zheng, C., and Guan, J. L. (2000) *J. Cell Biol.* **149,** 423–430
25. Brewer, G. J., Torricelli, J. R., Evege, E. K., and Price, P. J. (1993) *J. Neurosci. Res.* **35,** 567–576
26. Carlin, R. K., Grab, D. J., Cohen, R. S., and Siekevitz, P. (1980) *J. Cell Biol.* **86,** 831–845
27. Nakamura, H., and Funahashi, J. (2001) *Methods* **24,** 43–48
28. Lev, S., Moreno, H., Martinez, R., Canoll, P., Peles, E., Musacchio, J. M., Plowman, G. D., Rudy, B., and Schlessinger, J. (1995) *Nature* **376,** 737–745
29. Murata, Y., Hamada, S., Morishita, H., Mutoh, T., and Yagi, T. (2004) *J. Biol. Chem.* **279,** 49508–49516
30. Bonn, S., Seeburg, P. H., and Schwarz, M. K. (2007) *Mol. Cell. Biol.* **27,** 4121–4132
31. Mitra, S. K., Hanson, D. A., and Schlaepfer, D. D. (2005) *Nat. Rev. Mol. Cell. Biol.* **6,** 56–68
32. Mitra, S. K., and Schlaepfer, D. D. (2006) *Curr. Opin. Cell Biol.* **18,** 516–523
33. Klinghoffer, R. A., Sachsenmaier, C., Cooper, J. A., and Soriano, P. (1999) *EMBO J.* **18,** 2459–2471
34. Cohen, L. A., and Guan, J. L. (2005) *Curr. Cancer Drug Targets* **5,** 629–643
35. Lietha, D., Cai, X., Ceccarelli, D. F., Li, Y., Schaller, M. D., and Eck, M. J. (2007) *Cell* **129,** 1177–1187
36. Schaller, M. D., Hildebrand, J. D., Shannon, J. D., Fox, J. W., Vines, R. R., and Parsons, J. T. (1994) *Mol. Cell. Biol.* **14,** 1680–1688
37. Dikic, I., Tokiwa, G., Lev, S., Courtneidge, S. A., and Schlessinger, J. (1996) *Nature* **383,** 547–550
38. Emond, M. R., and Jontes, J. D. (2008) *Dev. Biol.* **321,** 175–187
39. Xiong, W., and Parsons, J. T. (1997) *J. Cell Biol.* **139,** 529–539
40. Girault, J. A., Costa, A., Derkinderen, P., Studler, J. M., and Toutant, M. (1999) *Trends Neurosci.* **22,** 257–263
41. Tian, D., Litvak, V., and Lev, S. (2000) *J. Neurosci.* **20,** 6478–6487
42. Liu, Y., Zhang, G., Gao, C., and Hou, X. (2001) *Brain Res.* **909,** 51–58
43. Okigaki, M., Davis, C., Falasca, M., Harroch, S., Felsenfeld, D. P., Sheetz, M. P., and Schlessinger, J. (2003) *Proc. Natl. Acad. Sci. U. S. A.* **100,** 10740–10745
44. Buckbinder, L., Crawford, D. T., Qi, H., Ke, H. Z., Olson, L. M., Long, K. R., Bonnette, P. C., Baumann, A. P., Hambor, J. E., Grasser, W. A., III, Pan, L. C., Owen, T. A., Luzzio, M. J., Hulford, C. A., Gebhard, D. F., Paralkar, V. M., Simmons, H. A., Kath, J. C., Roberts, W. G., Smock, S. L., Guzman-Perez, A., Brown, T. A., and Li, M. (2007) *Proc. Natl. Acad. Sci. U. S. A.* **104,** 10619–10624
45. Gil-Henn, H., Destaing, O., Sims, N. A., Aoki, K., Alles, N., Neff, L., Sanjay, A., Bruzzaniti, A., De Camilli, P., Baron, R., and Schlessinger, J. (2007) *J. Cell Biol.* **178,** 1053–1064
46. Liu, G., Beggs, H., Jurgensen, C., Park, H. T., Tang, H., Gorski, J., Jones, K. R., Reichardt, L. F., Wu, J., and Rao, Y. (2004) *Nat. Neurosci.* **7,** 1222–1232
47. Ren, X. R., Ming, G. L., Xie, Y., Hong, Y., Sun, D. M., Zhao, Z. Q., Feng, Z., Wang, Q., Shim, S., Chen, Z. F., Song, H. J., Mei, L., and Xiong, W. C. (2004) *Nat. Neurosci.* **7,** 1204–1212
48. Li, W., Lee, J., Vikis, H. G., Lee, S. H., Liu, G., Aurandt, J., Shen, T. L., Fearon, E. R., Guan, J. L., Han, M., Rao, Y., Hong, K., and Guan, K. L. (2004) *Nat. Neurosci.* **7,** 1213–1221
49. Robles, E., and Gomez, T. M. (2006) *Nat. Neurosci.* **9,** 1274–1283
50. Rico, B., Beggs, H. E., Schahin-Reed, D., Kimes, N., Schmidt, A., and Reichardt, L. F. (2004) *Nat. Neurosci.* **7,** 1059–1069